Journal of the Korean Physical Society, Vol. 63, No. 5, September 2013, pp. 996∼1000

Effective Surface Modification of a Germanium Layer by using an Atmospheric Pressure Plasma Jet with a Round Ended Nozzle

Min Kim, M. G. Kim, S. R. Kim, H. Y. Chung and J. G. Choi
Busanil Science High School, Busan 604-828, Korea

Hea Min Joh and T. H. Chung*
Plasma Laboratory, Department of Physics, Dong-A University, Busan 604-714, Korea

Hyung Soo Kim and Y. Kim
Nanoscale Semiconductor Laboratory, Department of Physics, Dong-A University, Busan 604-714, Korea

(Received 31 January 2013, in final form 13 June 2013)

We investigate the surface modification of a germanium epitaxial layer grown on a silicon substrate by means of an atmospheric-pressure plasma jet. The plasma jet contains a large density of highly reactive radicals, as confirmed by optical emission spectra. The plasma jet with a nozzle with a round end has a higher current level compared to cylindrical and pencil-shaped nozzles, indicating the usefulness of this plasma jet for semiconductor processing. Raman spectra reveal a significant modification of the germanium surface under exposure to an atmospheric pressure plasma jet even for 1 min. The first-order Raman peak at 320 cm^{-1} has an asymmetric shoulder on the low-frequency side, which can be attributed to amorphization/oxidation of the germanium layer due to highly reactive radicals. The rapid surface change under short-time exposure indicates the practicality of the plasma jet for semiconductor processing.

PACS numbers: 52.77.-j, 52.40.Hf, 68.55.ag
Keywords: Atmospheric-pressure plasma jet, Germanium, Raman spectroscopy, Oxidation
DOI: 10.3938/jkps.63.996

I. INTRODUCTION

The atmospheric pressure plasma jet (APPJ) has gained a great deal of attention due to its wide applications including biological, medical, and material processing applications [1]. Due to the short-lived free radicals, which induce apoptosis in tumor cells, the utilization of APPJ in cancer therapies has been actively pursued worldwide [2–5]. The localized APPJ provides an effective means for delivering a lethal dose to a tumor without affecting the surrounding healthy tissues. Besides biomedical applications, APPJ has attractive features for the surface modification of semiconductor materials. First, APPJ, as its name implies, does not require sophisticated vacuum equipments. Therefore, APPJ could be a cost-effective tool. Second, APPJ generates a plasma plume in open space, unlike low-pressure plasmas in coplanar electrodes, and can reduce the sustain voltage by minimizing its size. Additionally, APPJ can treat a large variety and amount of source materials and by controlling the gas flux, prevent impurities from being mixed into the process region. Therefore, APPJ equipped with a proper scanning stage can be applied to local oxidation/amorphization of semiconductor materials during ultra-large-scale integrated circuit (ULSI) processing. Finally, the temperature of APPJ is near room temperature, meaning that the temperature-induced effect on the underlying semiconductor structures fabricated during previous process steps is virtually absent during APPJ treatment. This feature is quite important because the conventional diffusion step requires high-temperature annealing, which smears the sharp interface of such subtle structures. In spite of its attractiveness, the research on the APPJ toward the surface modification of semiconductors has been relatively limited. Previous studies have usually focused on the modification of metals or plastics to change the surface to hydrophilic surface or to enhance the adhesion property [6,7]. APPJs were also utilized to deposit silicon-dioxide films [8, 9]. Also, self-organized nanostructures were observed on atmospheric-microplasma-exposed surfaces [10].

The surface of a germanium (Ge) layer is investigated to explore the effectiveness of APPJ treatment because Ge is promising for next-generation ULSI materials due to its higher electron/hole mobilities as compared to sil-

*E-mail: thchung@dau.ac.kr; Fax: +82-51-200-7232

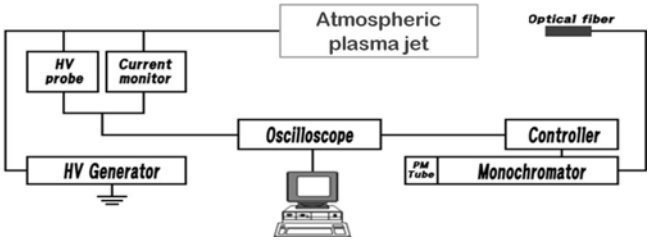

Fig. 1. Schematic diagram of the atmospheric-pressure plasma jet system.

icons [11]. In addition, germanium oxynitride is important for passivation and dielectric materials for Ge-based metal-oxide semiconductor field-effect transistors (MOSFETs) [12]. For biomedical applications of APPJ, a low level of current under moderate voltage is generally desirable. However, a higher level of current compared to biomedical applications may be required for effective semiconductor processing. Thus, we devised an APPJ device with a nozzle with round end, and that device carried a higher current at a given applied voltage. The degree of surface modification of the germanium layer was assessed by using micro Raman spectroscopy.

II. EXPERIMENTS

The plasma jet consists of a powered electrode, a teflon fitting, a quartz confinement tube, and a nozzle, as reported elsewhere [5]. A copper rod with wound wire acting as a powered electrode reduces the breakdown voltage and, thus, provides stable room-temperature operation. The discharge gas (helium) was fed through the tube at a flow rate of 2 SLM (standard liter per minute). The plasma was generated by using a pulsed bipolar source with a repetition frequency of several tens of kilohertz (EESYS APPS020). A typical operation condition of the plasma jet has an applied voltage of 1.9 kV_{rms} (root-mean-square value), a repetition frequency of 50 kHz, and a pulse width of 5.5 μs. The waveforms of the voltage and the current were measured using a real-time digital oscilloscope (LeCroy WS44XS-A) via a high voltage probe (Lecroy PPE20kV) and a current probe (Pearson 4100). To indentify the reactive species that are generated in the discharge, we measured the optical emission spectra in the range from 200 to 900 nm, as schematically shown in Fig. 1. The light emitted by the microplasma was focused by means of optical fiber into the entrance slit of a 0.75-m monochromator (SPEX 1702) equipped with a grating of 1200 groves per millimeter and a slit width of 100 μm.

In order to verify the general optical properties of this plasma jet, the optical emissions were measured as a function of time. A photosensor amplifier (Hamamatsu C6386-01) was used to observe the wavelength unresolved plasma emission.

The hydrogen-terminated Si substrates were first prepared by dipping in diluted HF solution. Subsequently, the epitaxial Ge layers were grown on the substrates by using a lamp-heated chemical vapor deposition (CVD) system. The growth condition was the same as reported previously [13]. Briefly, the growth temperature, times and pressure of the 1% hydrogen diluted GeH_4 source gas were 550 °C, 2 min and 5 min, and 60 Torr, respectively. The thicknesses of the Ge layers were about 200 nm and 500 nm, respectively.

The grown Ge layers were exposed to an APPJ from 1 to 30 min. After the exposure for 1 min, the color change of the exposed region is obvious even by visual inspection, indicating a significant change of refractive index. The diameter of the exposed region increased linearly, and the final diameter was about ∼3 mm after a 30-min exposure. The exposed surfaces were then examined by using micro Raman spectroscopy. The Raman spectrum was measured by using home-built equipment employing a modified fluorescence microscope (Olympus BX60) equipped with a Raman filter cube (Semrock) with an edge steepness less than 1 nm. A 488-nm Ar^+ laser (∼16 mW) was used as an excitation source. The laser power was measured using a handheld laser power meter (Coherent Lasercheck) underneath an objective lens. The Raman signal was collected through the microscope objective lens (Olympus ×50, numerical aperture = 0.75), which was used to focus the laser beam (spot diameter: ∼3.2 μm). The Raman signal was sent to 0.5-m monochromator with a 0.5-m focal length (Dongwoo optron DM500i) through a multimode optical fiber and was detected using a Peltier-cooled charge-coupled device (Andor iDus DV401A). An undoped Ge substrate was used as a reference.

III. DISCUSSION

Figures 2(a)-(c) illustrate the plasma plumes generated from three type of nozzles. Figure 2(a) is conventional nozzle (cylindrical nozzle). Figure 2(b) shows the nozzle with a tapered end (pencil-type nozzle). In our previous study, the pencil-type nozzle exhibited plasma stability while maintaining an efficient reaction chemistry and room temperature [14]. Thus, this type of nozzle is ideal for biomedical studies. Figure 2(c) shows the nozzle with a round end (round-type nozzle) devised for the present Ge modification. As shown in the figure, the plume length (∼3 cm) from the round-type nozzle is longer than those of the others and is tightly focused. Figure 2(d) shows a photograph of APPJ processing using a round-type nozzle. Figure 3(a) presents the voltage and current waveforms for the APPJ with a round-type nozzle. As shown in the figure 3(b), the cylindrical and the pencil-type nozzles exhibit almost equivalent current-voltage characteristics while the current from the round-type nozzle is approximately 10% higher than those of

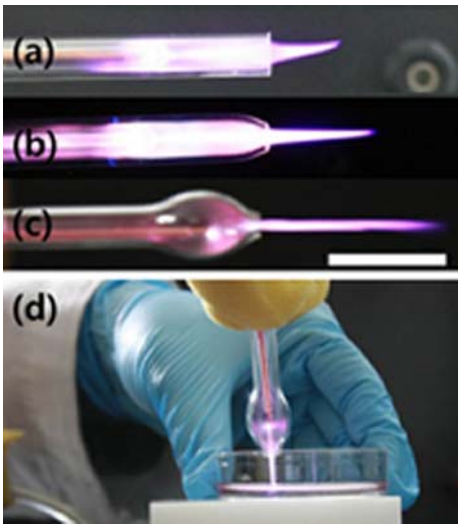

Fig. 2. (Color online) Photographs of plumes generated in a plasma jet with (a) a cylindrical nozzle, (b) a pencil-shaped nozzle, and (c) a round ended nozzle. (d) Photograph of the plasma treatment on semiconductor surface. The scale is 2 cm.

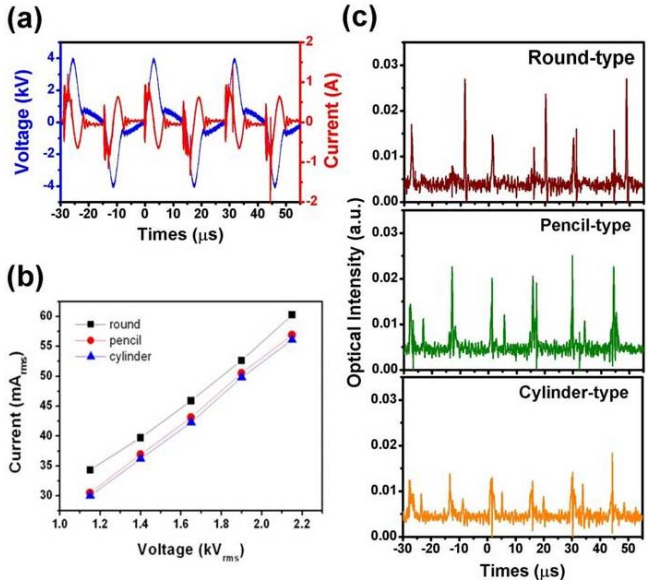

Fig. 3. (Color online) (a) Waveforms of voltage and current for the APPJ with round-ended nozzle, (b) current-voltage characteristics of the APPJs with three different types of nozzle, and (c) the temporal evolutions of wavelength-unresolved optical intensity for the APPJs with three different types of nozzle.

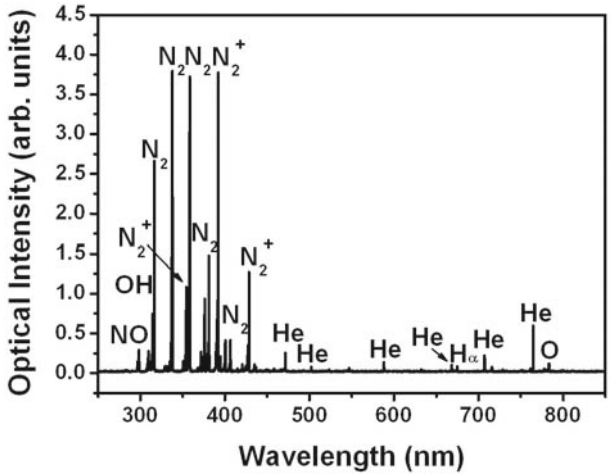

Fig. 4. Optical emission spectrum for the plume of a helium plasma jet with round ended nozzle.

the other two types of nozzle. The optical emission waveform from a photosensor amplifier was plotted for three different types of nozzle as shown in Fig. 3(c). The optical intensity is in phase with the current. Depending on the nozzle type, the plasma volume changes and the plasmas have different impedance. This modifies the current-voltage characteristics and optical emission intensity. A round-type nozzle jet has the largest optical intensity. The total current and optical emission intensity indicate that stronger plasmas are generated for the APPJ with a round-type nozzle. Probably, the round-type nozzle is not suitable for biomedical processing due to its higher current level. However, we anticipate that this type of nozzle will be adequate specifically for surface modification. The round end nozzle may provide a longer gas residence time for sufficient plasma activation. The plasma density is enhanced and the increase of conductivity leads to the increase in the conduction current. A sudden change in the geometrical shape in the gas flow path usually leads to the onset of a vortex gas flow pattern [15]. Plasma species circulate in the vortex formed in the round end for a long time and provoke the generation of other reactive species. This could be a desired environment for most of materials processing.

Figure 4 shows the emission spectrum observed in the plasma jet. The presence of excited helium, atomic oxygen, and some excited molecules can be confirmed even without additive gas such as oxygen. The strong emission at 391 nm is the $N_2{}^+$ line, and many strong nitrogen lines, an excited He atom line at 706.5 nm, and an excited oxygen line at 777 nm can be observed. The appearances of the nitrogen-oxide (NO) line at 282 nm and the H_α line at 656 nm are noted. Highly-reactive radicals, such as NO, O, and H, may be responsible for the surface modification [8,9].

Figure 5(a) shows the Raman spectra observed from APPJ-treated surfaces for 200 nm-thick Ge layer. The sharp and symmetric Raman peaks at 300 cm^{-1} from the Ge substrate and the untreated Ge layer on Si are first-order Ge Raman peaks. The Raman peak from the untreated Ge layer is slighter broader than that from the Ge substrate. The peak with a full width at half maximum (FWHM) of ∼8 cm^{-1} reflects the high crystalline quality of the Ge layer. With exposure to an APPJ only for 1 min, the Raman peak at 300 cm^{-1} shows a dramatic change, acquiring an asymmetric shoulder on the

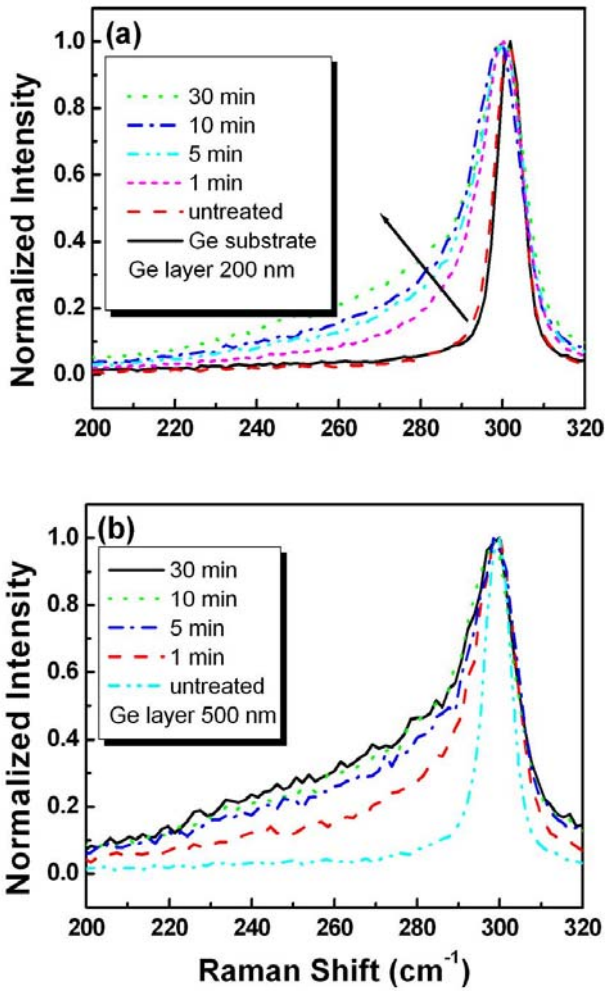

Fig. 5. (Color online) (a) Raman spectra of 200 nm-thick Ge layer for various plasma exposure times. The arrow indicates the direction of shoulder development with increasing plasma treatment time. (b) Raman spectra of 500 nm-thick Ge layer depending on the plasma exposure time.

low-frequency side. Concomitantly, the FWHM of the peak increases to 13.3 cm^{-1}. The development of the shoulder as indicated by the arrow, is more clearly observable with increasing plasma exposure time. The final FWHM reaches 17 cm^{-1} for a 30-min treatment. Figure 5(b) shows the Raman spectra observed from APPJ treated surfaces for 500 nm thick Ge layer. The spectra show the similar trend but the spectra are broader. Figure 6 summarizes the FWHMs of two Ge layers depending on the plasma exposure time. The FWHM tends to saturate for 500 nm thick Ge layer when exposed longer than 10 min. The final FWHM reaches 22 cm^{-1} for 30 min treatment. Noting that the amorphous Ge-Ge mode appears at 270 cm^{-1} [16], we can explain the asymmetric broadening caused by the APPJ exposure in terms of the formation of an amorphized/oxidized Ge layer. In addition, we noted the slight red shift (maximum shift: ∼4 cm^{-1}) of the Raman peak with increasing APPJ exposure time. This effect usually leads to a red shift in the Raman spectrum accompanied by a broadening of the peak. In addition, the stress between the remaining Ge and the germanium oxide may play a rule in the shift, presumably due to strain build-up.

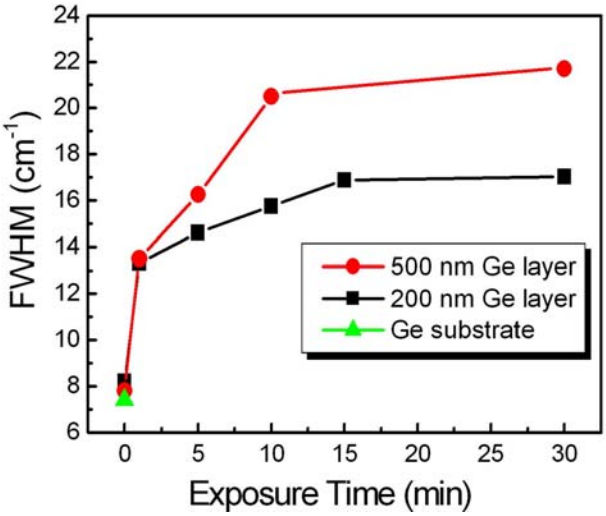

Fig. 6. (Color online) Full width at half maximum of Raman peak as a function of exposure time.

The chemical composition of the exposed region is not clear at present and certainly requires further study. However, as evidenced by the emission spectrum of the APPJ, the plasma contains a large density of NO, O, H free radicals. Therefore, this region is plausibly composed of germanium oxynitride and germanium crystallites. In the Si surface modification by using an APPJ, which is an efficient provider of atomic oxygen and nitrogen, fast oxidation, followed by fast diffusion of atomic oxygen/nitrogen in the SiO_2 matrix, has been reported [17]. To our best knowledge, there is no report on the surface modification of Ge by using an APPJ. However, a similar mechanism may hold for Ge modification. Noting that the bond strength of the Ge lattice is lower than that of the Si lattice, the oxidation/nitridation of Ge under an APPJ should be faster. To account for the broader Raman spectra for thicker Ge layer, several possibilities could be suggested. First, as reported in our previous work, thick Ge layer is relaxed being accompanied with the generation of large density threading dislocations [8]. The threading dislocations may offer the effective oxidation/nitridation channels. Second, the oxidation/nitridation depth may be limited with Ge layer because Si with higher bond strength is plasma oxidation/nitridation resistant. This means that in-depth oxidation does not proceed further for thin Ge layer and the lateral oxidation may be promoted instead. The Ge modification depth is expected to be in the sub-micron range. In this case, a minor change in the APPJ parameters could lead to a significant change in the Ge surface modification during APPJ scanning. Therefore,

the APPJ is more useful for Ge modification in a localized area rather than an entire wafer. The temporal stability of the APPJ in terms of the plume length and the radical generation rate could be issues for the adaptation of APPJ for a practical semiconductor processing. An APPJ scanning apparatus for the modification of a targeted area is under development in our laboratory.

IV. CONCLUSION

In conclusion, the APPJs with three types of nozzles were investigated. Among them, the APPJ with the round ended nozzle showed higher levels of electric current and optical intensity and longer plume length at a given voltage. Thus APPJ with a round-type nozzle is suitable for semiconductor processing. The surface modification by APPJ exposure for various time durations on a Ge layer grown by using CVD was investigated. The Ge Raman peak was asymmetrically broadened only for a 1-min exposure. This result indicates that a short-time exposure is sufficient for surface modification. Thus, this feature demonstrates the practicality and suitability of the APPJ with a round-type nozzle for semiconductor processing.

ACKNOWLEDGMENTS

This work is partially supported by the research and education program through the Korea Foundation for the Advancement of Science and Creativity (KOFAC) funded by the Ministry of Education, Science and Technology. HMJ and THC would like to gratefully acknowledge support by the Basic Science Research Program through the National Research Foundation of Korea (NRF) funded by the Ministry of Education, Science and Technology (2012 R1A1A2002591). HSK and YK acknowledge the financial support by the Basic Science Research Program through the National Research Foundation of Korea (NRF) funded by the Ministry of Education, Science and Technology (2012R1A1A2002076).

REFERENCES

[1] M. Laroussi and T. Akan, Plasma Process. Polym. **4**, 777 (2007).
[2] J. Y. Kim, Y. Wei, J. Li, P. Foy, T. Hawkins, J. Ballato and S. O. Kim, Small **7**, 2291 (2011).
[3] S. J. Kim, T. H. Chung, S. H. Bae and S. H. Leem, Appl. Phys. Lett. **97**, 023702 (2010).
[4] G. J. Kim, W. Kim, K. T. Kim and J. K. Lee, Appl. Phys. Lett. **96**, 021502 (2010).
[5] H. M. Joh, S. J. Kim, T. H. Chung and S. H. Leem, Appl. Phys. Lett. **101**, 053703 (2012).
[6] M. C. Kim, D. K. Song, H. S. Shin, SH. Baeg, G. S. Kim, JH. Boo, J. G. Han and S. H. Yang, Surf. Coat. Tech. **172**, 312 (2003).
[7] M. Noeske, J. Degenhardt, S. Strudthoff and U. Lommatzsch, Int. J. Adhes. **24**, 171 (2004).
[8] S. E. Babayan, J. Y. Jeong, V. J. Tu, J. Park, G. S. Selwyn and R. F. Hicks, Plasma Sources Sci. Technol. **7**, 286 (1998).
[9] V. Raballand, J. Benedikt and A. von Keudell, Appl. Phys. Lett. **92**, 091501 (2008).
[10] D. Mariotti, V. Svrcek and D. G. Kim, Appl. Phys. Lett. **91**, 183111 (2007).
[11] S. M. Sze, *Physics of Semiconductor Devices* (Wiley, New York, 1981).
[12] C. O. Chui and Saraswat, IEEE EDL. **53**, 1501 (2006).
[13] J. H. Kim, S. R. Moon, H. S. Yoon, J. H. Jung, Y. Kim, Z. G. Chen, J. Zou, D. Y. Choi, H. J. Joyce, Q. Gao, H. H. Tan and C. Jagadish, Cryt. Growth Des. **12**, 135 (2012).
[14] S. J. Kim, T. H. Chung and S. H. Bae, Phys. Plasma **17**, 053054 (2010).
[15] M. Ohring, *Materials Science of Thin Films* (Academic Press, London, 2002).
[16] M. Zacharias, R. Weigand, B. Dietrich, F. Stolze and J. Blasing, J. Appl. Phys. **81**, 2382 (1997).
[17] H. Kakiuchi, H. Ohmi, M. Harada, H. Watanabe and K. Yasutake, Appl. Phys. Lett. **90**, 091909 (2007).
[18] J. H. Jung, H. S. Yoon, Y. L. Kim, M. S. Song, Y. Kim, Z. G. Chen, J. Zou, D. Y. Choi, J. H. Kang, H. J. Joyce, H. H. Tan and C. Jagadish, Nanotechnology **21**, 295602 (2010).